AIP Advances

Bulk Mn-Al-C permanent magnets prepared by various techniques

Rajasekhar Madugundo, Ozlem Koylu-Alkan, and George C. Hadjipanayis

Citation: AIP Advances **6**, 056009 (2016); doi: 10.1063/1.4943242
View online: http://dx.doi.org/10.1063/1.4943242
View Table of Contents: http://scitation.aip.org/content/aip/journal/adva/6/5?ver=pdfcov
Published by the AIP Publishing

AIP ADVANCES **6**, 056009 (2016)

Bulk Mn-Al-C permanent magnets prepared by various techniques

Rajasekhar Madugundo,[a] Ozlem Koylu-Alkan, and George C. Hadjipanayis[a]
Department of Physics and Astronomy, University of Delaware, Newark, DE, 19716, USA

(Presented 13 January 2016; received 5 November 2015; accepted 15 December 2015; published online 1 March 2016)

Bulk Mn-Al-C magnets have been prepared by hot-compaction, microwave sintering and hot-deformation. Powders of $Mn_{53.5}Al_{44.5}C_2$ alloy in the ε-phase produced by high energy ball milling have been used as precursor for the hot-compacted and microwave sintered magnets. Hot-deformed magnets were produced from alloy pieces in the τ-phase. The hot-compacted magnet exhibits magnetization, remanence and coercivity of 50 emu/g, 28 emu/g and 3.3 kOe, respectively. Microwave sintered magnet shows a maximum magnetization of 94 emu/g, remanence of 30 emu/g and coercivity of 1.1 kOe. The best magnetic properties are obtained in hot-deformed magnets with magnetization, remanence, coercivity and energy product of 82 emu/g, 50 emu/g, 2.2 kOe and 1.8 MGOe, respectively. Hot-deformed magnets exhibit texture with the highest degree of texture obtained 0.26. It is found that the pressure applied during compaction/deformation favors coercivity. [http://dx.doi.org/10.1063/1.4943242]

I. INTRODUCTION

Volatile rare-earth (RE) metal prices, environmental concerns involving the RE-metal extraction, and geopolitical issues joined by the large coercivity (H_c) gap existing between alnico/ferrite-based magnets and RE-based magnets created a need to reinvestigate the Mn-Al based magnets, first reported by Koch *et al*. in 1960, for the development of a non-rare earth magnet competing with the medium performance Nd-Fe-B magnets.[1–3] The hard-magnetic properties in Mn-Al alloy system originate from the $L1_0$ τ-phase with high anisotropy field of ~40 kOe, a relatively high saturation magnetization of ~96 emu/g and Curie temperature > 300 °C.[1–3] The Mn-Al magnet with best properties so far was produced by Matsushita Electrical Industrial company (M_r = 6.1 kG, H_c = 3.2 kOe, $(BH)_{max}$ ~7 MGOe) by hot extrusion/swaging.[4] However, the performance improvement as compared to the ferrite magnets was not sufficient to justify the cost of the manufacturing. Furthermore, the invention of RE-based magnets ($RECo_5$) in the 1960's shifted the research interests off from Mn-Al.[1,5,6] The very recent renewed interest in Mn-Al alloys resulted in a number of investigations that explored various processing techniques. The τ-MnAl phase is metastable, and is usually formed by quenching from the high temperature hcp ε-phase followed by annealing at temperatures between 500-700 °C.[3,4] Prolonged annealing results in decomposition of the τ-MnAl phase to the equilibrium β-Mn and γ_2-Al_8Mn_5 phases.[3] Addition of a small amount of C slows down the decomposition of the τ-phase and increases H_c.[4] Various techniques such as mechanical milling,[7,8] mechanical alloying,[9,10] melt-spinning,[11,12] gas atomization,[13] spark erosion[14] were used to make base material (powder) which then was consolidated to make bulk magnets by spark plasma sintering[15] and equal channel angular extrusion.[16] Unfortunately, all the results reported so far are very inferior compared to the properties reported by Ohtani *et al*.[4] Though the powders exhibited high coercivity (>4.8 kOe),[17] the magnetization was significantly lower and the consolidated bulk magnets showed a further decrease in magnetization and coercivity as well. In the present study, we

[a]Author to whom correspondence should be addressed. Electronic mail: mraja@udel.edu, hadji@udel.edu

have explored different techniques (hot-compaction, microwave sintering and hot-deformation) to produce Mn-Al based bulk magnets with improved properties.

II. EXPERIMENTAL DETAILS

An alloy with nominal composition $Mn_{53.5}Al_{44.5}C_2$ was prepared by arc-melting the pure elements. The melting process was repeated 4 times to ensure better homogeneity. To compensate for the Mn losses during the melting, an excess of 3% was added. Small cubes of C with dimension ~1 x 1 x 1 mm^3 were used so that the cubes dissolve easily in the molten alloy. High energy ball milling, microwave (MW) sintering, hot-compaction and hot-deformation techniques were employed to produce bulk magnets. The arc-melted ingot pieces were homogenized at 1100 °C for 20 hours followed by water quenching and tempering ($\varepsilon \rightarrow \tau$ phase transformation) at 550 °C for 20 min. The tempered pieces were crushed to powders with particle size <250 μm. The powder was high energy ball milled (HEBM) with 1:10 powder to ball ratio for 2 h. The milled powder was heat-treated again at 550 °C for 10 min. For hot-compaction and MW-sintering, the powders were produced by HEBM of ingot pieces homogenized at 1100 °C for 20 hours to obtain the ε-phase as described above. The HEBM powder was hot-compacted at 700 °C into the shape of a cylinder 10 mm in diameter and 5 mm in height by applying a uniaxial pressure of 275 MPa with tungsten carbide (WC) punches. For MW-sintering, green compact was made from the powder with dimensions 5 x 5 x 4 mm^3 by applying 1.2 GPa pressure. The green compact was MW-sintered at 700 °C for 10 min under argon atmosphere in a Gerling microwave sintering system (2.45 GHz, 1800 watt). The MW sintered sample was heat-treated at 600 °C for 10 min. Hot-deformation was performed on the alloy sample with the τ-phase, i.e. on the tempered alloy. An alloy piece of 5x5x7 mm^3 was hot-deformed using WC punches to 75% of its original height. The deformation was performed at 700 °C by applying uniaxial pressure using WC punches allowing the deformed material to expand freely in the plane perpendicular to the deformation direction. The magnetic properties of the samples were measured by a vibrating sample magnetometer at room temperature. A maximum field of 30 kOe was applied during the measurements and the hysteresis loops were corrected for the self-demagnetization effect.[18] Phase analyses were studied by X-ray diffraction (XRD) using a Rigaku Ultima IV instrument with Cu Kα radiation. Microstructure studies were performed using a JEOL (JSM-6335F) scanning electron microscope (SEM). The density of samples was measured by the Archimedes method.

III. RESULTS AND DISCUSSION

Hysteresis loops of the HEBM powders as-milled for 2 h and post mill heat-treated at 550 °C for 10 min are shown in Fig. 1. The milling time was chosen to be 2 h as milling for longer hours

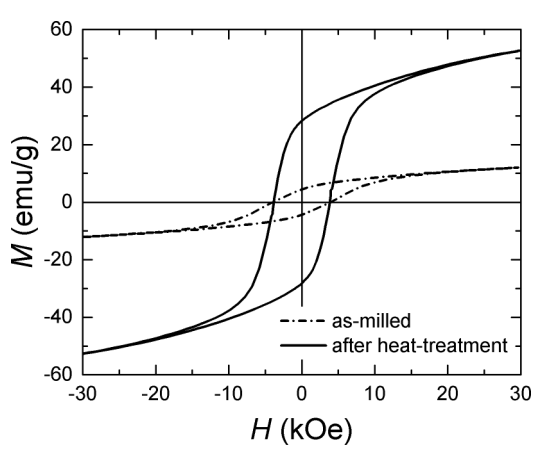

FIG. 1. Hysteresis loops of $Mn_{53.5}Al_{44.5}C_2$ HEBM powders (a) as-milled (b) annealed at 550 °C for 10 min.

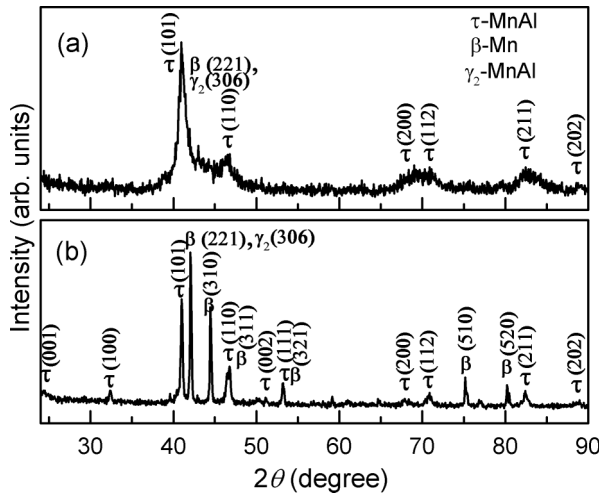

FIG. 2. XRD patterns of $Mn_{53.5}Al_{44.5}C_2$ powders (a) as HEBM for 2 h and (b) after heat-treatment at 550 °C for 10 min.

induces formation of the non-magnetic β- and γ_2-phases.[3] The as-milled powder shows $M_{/30\,\mathrm{kOe}}$, M_r and H_c values of 12 emu/g, 5 emu/g and 3.9 kOe, respectively. After the heat-treatment $M_{/30\,\mathrm{kOe}}$ and M_r increased to 53 and 28 emu/g, respectively, whereas the H_c value remained unchanged. Figure 2 shows the XRD patterns of the as-milled and heat-treated powders. XRD pattern of the as-milled powder shows peaks mainly arising from the τ-phase along with smaller peaks from the β- and γ_2-phases. Broadening of the peaks is caused by the decreased particle/grain size and the stress induced during the milling process. The lower magnetization of as-milled powders is possibly due to the disordered structure induced by the stress. The XRD patterns of the heat-treated powder show peaks belonging to τ-, β- and γ_2-phases and sharper peaks indicating grain growth and stress relief, that cause an increase in magnetization after the heat-treatment. The τ-phase quantity decreased due do decomposition to the β- and γ_2-phases.

Bulk magnets were produced by hot-compaction, MW-sintering and hot-deformation processes. For hot-compaction and MW-sintering, the starting material was a powder in ε-phase. Figure 3 shows the hysteresis loops of magnets produced by these three processes and the properties are listed in Table I. The hot-compacted magnet exhibits $M_{/30\,\mathrm{kOe}}$, M_r, H_c and $(BH)_{max}$ of 50 emu/g, 28 emu/g, 3.3 kOe and 0.6 MGOe, respectively. The density of the magnet is found to be 4.9 g/cc. Hysteresis loops of MW as-sintered magnet and after heat-treatment at 600 °C for 10 min are shown in Fig. 3(b). The as-sintered magnet shows $M_{/30\,\mathrm{kOe}}$, M_r and H_c of 56 emu/g, 20 emu/g and 1.1 kOe, respectively. After the heat-treatment, the $M_{/30\,\mathrm{kOe}}$ is increased significantly from 56 to 94 emu/g and M_r from 20 to 39 emu/g while H_c remained unchanged. The density is estimated to be 4.1 g/cc and the $(BH)_{max}$ of the magnet after heat-treatment is 0.5 MGOe. The hot-deformed magnets exhibit texture in the magnetic properties. Figure 3(c) shows the hysteresis loops of the hot-deformed magnet measured with applied field parallel to the deformation direction ($\|^{el}$) and perpendicular to the deformation direction ($\perp^{er}$). When measured in the $\|^{el}$ direction the $M_{/30\,\mathrm{kOe}}$, M_r and H_c are measured to be 79 emu/g, 36 emu/g and 2.7 kOe, respectively and when measured in $\perp^{er}$ direction 82 emu/g, 50 emu/g and 2.2 kOe, respectively. The density of the hot-deformed magnet is 5.2 g/cc, which is 100% of the bulk value. A $(BH)_{max}$ of 1.8 MGOe has been obtained from the loop measured in $\perp^{er}$ direction. The anisotropy in the properties is attributed to the texture developed during the hot-deformation stage. The degree of texture is estimated by calculating texture parameter (tp) from M_r values measured in $\perp^{er}$ and $\|^{el}$ direction using the formula, $tp = (M_r^{\perp} - M_r^{\|})/M_r^{\perp}$. The value of tp is 1 for fully textured material and 0 for isotropic one.[19] The tp for the hot-deformed magnet is calculated to be 0.26 and the texture developed is in the plane perpendicular to the deformation direction. In the case of Mn-Al-C magnets prepared by extrusion, Koch *et al.*,[1] Ohtani *et al.*,[4] Sakamoto *et al.*[20] and Bittner *et al.*[19] reported texture formation in the axis parallel to the extrusion direction.

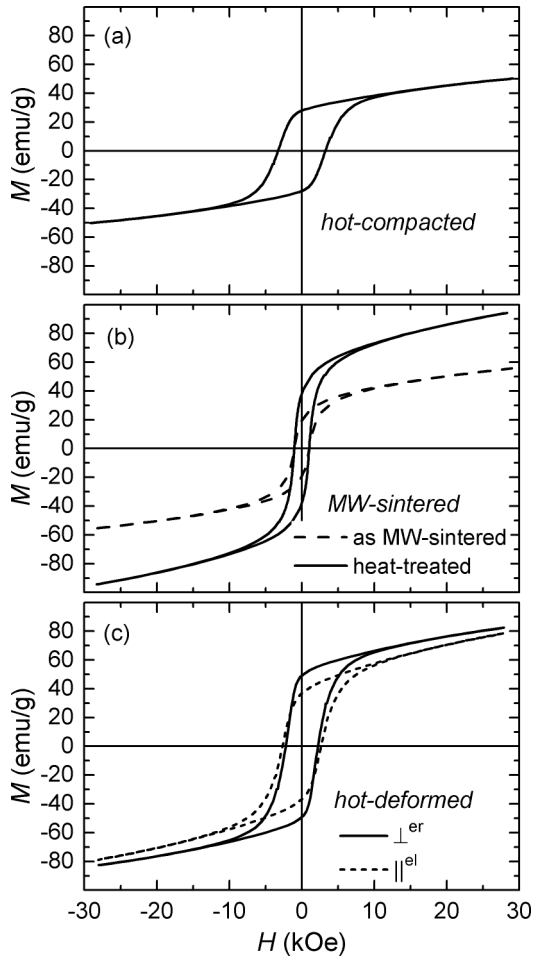

FIG. 3. Hysteresis loops of $Mn_{53.5}Al_{44.5}C_2$ magnets produced by (a) hot-compaction, (b) MW-sintering and (c) hot-deformation processes.

Figure 4 shows the XRD patterns of the magnets prepared by the three processes. The XRD pattern of hot-compacted magnet (Fig. 4(a)) shows peaks belonging to τ-, β- and γ_2-phases. From the XRD pattern it can also be seen that the quantity of the β- and γ_2-phases is significantly high explaining the relatively low magnetization in this sample. The higher temperature used for hot-compaction for relatively longer time (time to heat from RT to 700 °C and compaction together was ~22 min) could be a reason for the excessive decomposition of the τ-phase into β- and γ_2-phases. From the XRD patterns of MW-sintered magnet shown in Fig. 4(b), it can be seen that the sample retained the majority of its τ-phase and only minor peaks from β- and γ_2-phases are observed. Faster heating from RT to 700 °C due to the higher heating rates achievable in MW-sintering minimizes the τ-phase decomposition into β- and γ_2-phases. The XRD patterns of the hot-deformed magnet

TABLE I. Magnetic properties of $Mn_{53.5}Al_{44.5}C_2$ magnets produced by hot-compaction, MW-sintering and hot-deformation along with density values. The properties reported for hot-deformed magnet were measured in $\perp^{er}$ to the deformation direction.

Process	$M_{s/30\,kOe}$ (kG)	$M_{r/30\,kOe}$ (kG)	$H_{c/30\,kOe}$ (kOe)	$(BH)_{max}$ (MGOe)	ρ (g/cc)
Hot-compacted	50	28	3.3	0.6	4.9
MW-sintered	94	39	1.1	0.5	4.1
Hot-deformed	82	50	2.2	1.8	5.2

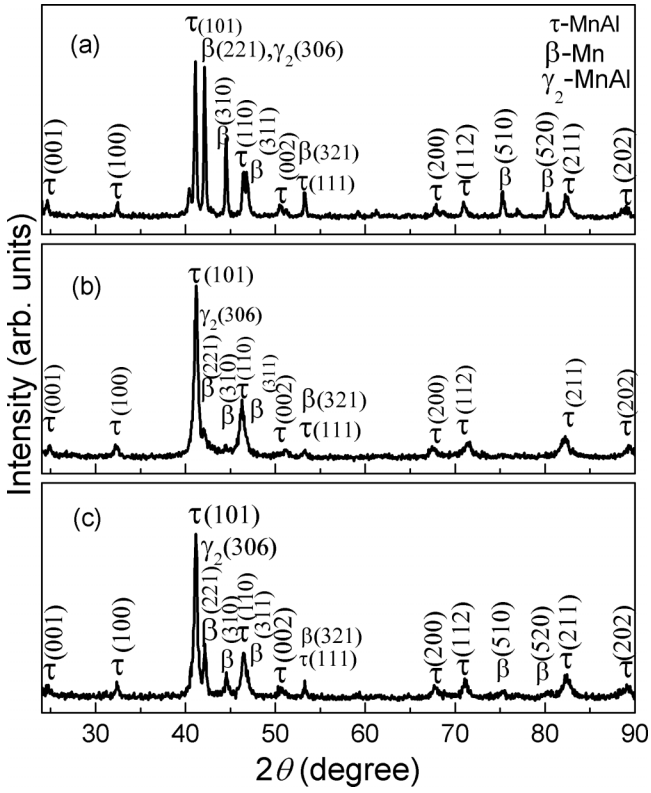

FIG. 4. XRD patterns of $Mn_{53.5}Al_{44.5}C_2$ magnets produced by (a) hot-compaction, (b) MW-sintering followed by heat-treatment and (c) hot-deformation processes.

(Fig. 4(c)) show the majority of the sample to be in the τ-phase. The smaller H_c of 1.1 kOe obtained compared to 3.3 kOe in the hot-compacted magnet even though the starting powder was the same for both the processes could not be understood. From the H_c values observed in the magnets prepared by hot-compaction and hot-deformation where the pressure is applied during compaction and deformation, respectively, it can be said that the pressure has an effect on coercivity in the Mn-Al alloy system. The Mn-Al-(C) magnets with highest H_c reported so far was also prepared by hot-extrusion where significant amount of pressure was involved.[4]

The SEM secondary images of the hot-compacted, MW-sintered followed by heat-treatment at 600 °C for 10 min and hot-deformed magnets are shown in Fig. 5. The microstructure of hot-compacted and MW-sintered show somewhat bigger grains compared to that of hot-deformed magnet. The microstructure of the MW-sintered magnet shows emergence of a twin-like morphology during the ε → τ transformation due to the strain associated with it.[19] This kind of twin-like features are not observed in the microstructure of the hot-compacted magnet. Microstructure of the

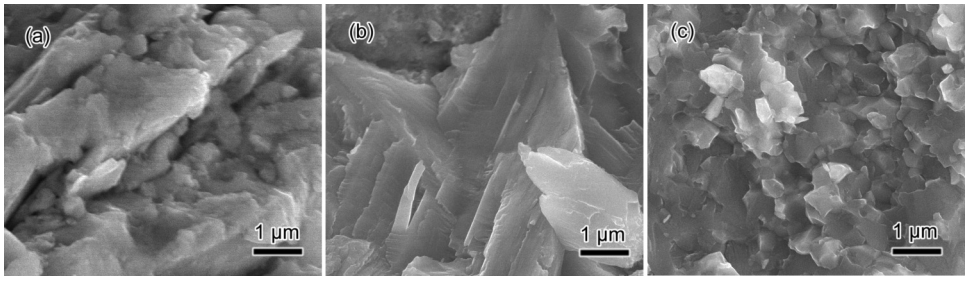

FIG. 5. SEM secondary electron images taken on the fractured surface of (a) hot-compacted, (b) MW-sintered and heat-treated and (c) hot-deformed magnets.

hot-deformed magnet shows much refined grains (<500 nm) caused by the dynamic recrystallization that occurs during the hot-deformation.[19] The relatively high coercivity in hot-deformed magnet can be attributed to the refined grain size possibly due to pinning of domain walls at the grain boundaries. The other possible contribution to the increase in coercivity is the absence of antiphase boundaries in hot-deformed samples.[21] However, the coercivity difference between the hot-compacted and MW-sintered magnets could not be correlated to the microstructure obtained by SEM. Further TEM studies are underway to understand the coercivity mechanism in the Mn-Al magnets.

IV. CONCLUSIONS

We have prepared bulk Mn-Al-C magnets by using three different techniques of hot-compaction, MW-sintering and hot-deformation. The $Mn_{53.5}Al_{44.5}C_2$ alloy powder produced by high energy ball milling in ε-phase was used as precursor for the hot-compaction and microwave sintering. Hot-deformation was performed on alloy pieces with the τ-phase. Hot-compacted magnet exhibits magnetization, remanence and coercivity of 50 emu/g, 28 emu/g and 3.3 kOe, respectively. Microwave sintered magnet shows a higher magnetization of 94 emu/g, remanence of 30 emu/g but a lower coercivity of 1.1 kOe. The optimum magnetic properties were obtained in hot-deformed magnets with magnetization, remanence and coercivity of 82 emu/g, 50 emu/g and 2.2 kOe, respectively. Hot-deformed magnets exhibit anisotropy due to the texture developed during the deformation. Pressure applied during the compaction/deformation was found to favor the coercivity.

ACKNOWLEDGEMENTS

The project was funded by U. S. Department of Energy (DE-FG02-90ER45413) and National Science Foundation (NSF G-8). The authors would like to thank Daniel C. Neil for his help in conducting MW-sintering experiment.

[1] A.J.J. Koch, P. Hokkeling, M.G. v. d. Steeg, and K.J. de Vos, J. Appl. Phys. **31**, S75 (1960).
[2] L. Pareti, F. Bolzoni, F. Leccabue, and A.E. Ermakov, J. Appl. Phys. **59**, 3824 (1986).
[3] H. Kōno, J. Phys. Soc. Japan **13**, 1444 (1958).
[4] T. Ohtani, N. Kato, S. Kojima, K. Kojima, Y. Sakamoto, I. Konno, M. Tsukahara, and T. Kubo, IEEE Trans. Magn. **13**, 1328 (1977).
[5] J.M.D. Coey, J. Phys. Condens. Matter **26**, 064211 (2014).
[6] D. Niarchos, G. Giannopoulos, M. Gjoka, C. Sarafidis, V. Psycharis, J. Rusz, A. Edström, O. Eriksson, P. Toson, J. Fidler, E. Anagnostopoulou, U. Sanyal, F. Ott, L.-M. Lacroix, G. Viau, C. Bran, M. Vazquez, L. Reichel, L. Schultz, and S. Fähler, JOM **67**, 1318 (2015).
[7] Q. Zeng, I. Baker, and Z.C. Yan, J. Appl. Phys. **99**, 44 (2006).
[8] H. Jian, K.P. Skokov, and O. Gutfleisch, J. Alloys Compd. **622**, 524 (2015).
[9] T. Saito, J. Appl. Phys. **93**, 8686 (2003).
[10] O. Obi, L. Burns, Y. Chen, T. Fitchorov, S. Kim, K. Hsu, D. Heiman, L.H. Lewis, and V.G. Harris, J. Alloys Compd. **582**, 598 (2014).
[11] Y. Geng, M.J. Lucis, P. Rasmussen, and J.E. Shield, J. Appl. Phys. **118**, 033905 (2015).
[12] J.M. Le Breton, J. Bran, E. Folcke, M. Lucis, R. Larde, M. Jean, and J.E. Shield, J. Alloys Compd. **581**, 86 (2013).
[13] A. Chaturvedi, R. Yaqub, and I. Baker, J. Phys. Condens. Matter **26**, 064201 (2014).
[14] a. E. Berkowitz, J.D. Livingston, and J.L. Walter, J. Appl. Phys. **55**, 2106 (1984).
[15] P. Saravanan, V.T.P. Vinod, M. Černík, a. Selvapriya, D. Chakravarty, and S.V. Kamat, J. Magn. Magn. Mater. **374**, 427 (2015).
[16] A. Chaturvedi, R. Yaqub, and I. Baker, Metals (Basel) **4**, 20 (2014).
[17] Q. Zeng, I. Baker, J.B. Cui, and Z.C. Yan, J. Magn. Magn. Mater. **308**, 214 (2007).
[18] A. Aharoni, J. Appl. Phys. **83**, 3432 (1998).
[19] F. Bittner, L. Schultz, and T.G. Woodcock, Acta Mater. **101**, 48 (2015).
[20] Y. Sakamoto, S. Kojima, K. Kojima, T. Ohtani, and T. Kubo, J. Appl. Phys. **50**, 2355 (1979).
[21] E.L. Houseman and J.P. Jakubovics, J. Magn. Magn. Mater. **31-34**, 1007 (1983).